# An Analysis of the Tolerance to Crosstalk Noise of a Pulse Width Modulation System

This paper reports the results of an investigation to determine the drive degradation caused by random noise in a pulse width modulation (PWM) system originally designed for communicating on coaxial cable but using instead twisted-pair cables. Presented are the analysis of the driver/receiver circuit, the theoretical modeling of the transmitted waveforms over the twisted-pair medium using ASTAP, and a methodology for trading off rms noise for transmission capability. The analysis of the effect of noise on drive distance as a function of allowable error rate is derived, and an example is provided. Finally, a simplified analysis technique is proposed to allow rapid calculation of approximate (yet conservative) results.

#### 1. Introduction

A study was undertaken to determine the effects of substituting multiple twisted-pair cable for the coaxial cable presently being used to carry pulse width modulated (PWM) data signals for IBM display products. The analysis was simulated using ASTAP, the advanced statistical analysis program [1], first for the coaxial cable (to verify that the analysis was correct by showing the design to be within specifications) and then for the twisted-pair cable. Experimental verification of our results are in progress and are thus not included here.

The technical issues addressed by this investigation include how a display product performs on this different medium, and how susceptible it is to the types of electrical noises which are expected on this type of cable. The results of an engineering study to address these issues are described. An analysis of the driver/receiver circuit is presented with an emphasis on pulse distortion in the twisted-pair medium, and pulse width variation over the parameter ranges. The effect of noise on the pulse width is then computed. Finally, a simplifying and slightly conservative approach is presented to facilitate making the requisite trade-offs.

#### 2. Analysis of the driver/receiver circuit

A simplified diagram of the driver/receiver for a typical IBM display terminal is shown in Fig. 1. The circuit for each

driver/receiver consists of two solid logic technology (SLT) modules, three resistor-capacitor packs, and five discrete components. Not shown are the baluns at each end of the transmission line which provide impedance matching and common mode noise rejection, and prevent ground loops. The circuit operation is described next.

With inputs  $A_1$  and  $A_2$  low, transistors  $Q_1$  and  $Q_2$  are cut off and the cable is charged to about 7.4 V. When a positive level is applied at  $A_1$ ,  $Q_1$  saturates and pulls the cable voltage to ground potential.

 $R_1$  matches the cable impedance and provides a current path to one side of a differential amplifier. The other side of the differential amplifier is connected to a reference voltage  $V_{\rm ref}$  created by the voltage divider resistors  $R_2$  and  $R_3$ .

Data transmission is via PWM signals at a bit rate of approximately 1.2 Mb/s. Typical receiver pulse width specifications are as follows: A *I* bit must be greater than 620 ns and less than or equal to 670 ns, with a nominal specification of 630 ns. A *0* bit must be greater than 190 ns and less than or equal to 250 ns, with a nominal pulse width of 210 ns. The driver/receiver was designed to transmit signals through a maximum of 610 m (2000 feet) of coaxial cable.

© Copyright 1983 by International Business Machines Corporation. Copying in printed form for private use is permitted without payment of royalty provided that (1) each reproduction is done without alteration and (2) the Journal reference and IBM copyright notice are included on the first page. The title and abstract, but no other portions, of this paper may be copied or distributed royalty free without further permission by computer-based and other information-service systems. Permission to republish any other portion of this paper must be obtained from the Editor

The next section describes the ASTAP simulation used to determine the effect of crosstalk noise in this pulse width modulation system.

## 3. Simulation of the effect of the media on the signal

ASTAP simulation was used to model No. 22 gauge twisted copper cable, as well as the driver and receiver circuit shown in Fig. 1. Analysis was also done after replacing the No. 22 gauge solid copper twisted-pair wire with coaxial cable. ASTAP was run in order to define the limitations of twisted copper cable for these drive conditions, determine the sensitivity of the circuit to crosstalk noise, and establish a basis for determining error rate as a function of input noise level.

The following cable characteristics were required in the simulation:

- Characteristic admittance of twisted copper cable,
- Attenuation per unit length,
- Inductance per unit length, and
- Capacitance per unit length.

An examination of Fig. 1 shows that the critical parameters in the determination of the transmitted voltage level and the detection threshold level are the power supply tolerances and the ratio of the voltage divider resistors  $R_2$  and  $R_3$ . Since the power supply variation is  $\pm 12\%$ , and  $R_2$  and  $R_3$  are held to  $\pm 1\%$ , the effect of resistor variation as well as the variation of the noncritical circuit components can be ignored in determining noise sensitivity as a function of parameter variation. The actual pulse width specification is based on worst-case transistors in the driver and receiver, so variations in the transistor parameters need not be separately accounted for. In order to determine the worst-case power supplies for signal detection, four ASTAP runs were made at the extremes of the power supply ranges in the receiver and driver, as shown in Table 1.

The resulting ASTAP simulation provided the pulse width variation as a function of power supply settings. For this configuration, the worst-case condition occurred with the driver power supply low (7.04 V) and the receiver power supply high (8.96 V).

In order to confirm the model, an ASTAP simulation was run with twisted copper cable replaced by 610 m of coaxial cable (the specification condition for a display terminal). The output waveforms were compared against the required pulse widths. Since the pulse width of signals received through the coaxial cable just met the interface information specification, the model was considered confirmed.

ASTAP simulations were then run for cable lengths from 65 m to 175 m in 5-m increments, with a driving signal

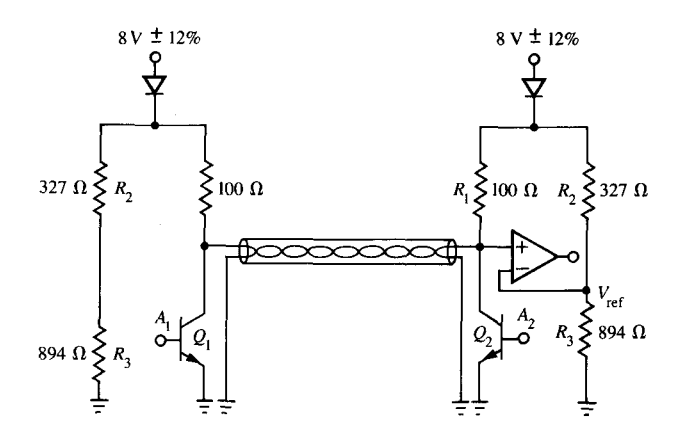


Figure 1 Typical display terminal driver/receiver circuit.

Table 1 Power supply limit conditions.

	Power supply of driver (V)	Power supply of receiver (V)	
1.	7.04	7.04	
2.	7.04	8.96	
3.	8.96	7.04	
4.	8.96	8.96	

consisting of a string of random 1 and 0 bits to determine maximum drive length with worst-case intersymbol interference. The first failing condition was reached for a 1 bit exceeding the maximum pulse width specification. The pattern preceding the 1 bit, 001, was chosen because it produced the worst-case intersymbol interference, i.e., the largest increase in pulse width. Figure 2 shows the waveform for this worst-case 1 bit at the end of 150 m of cable. Figure 3 is a graph showing the pulse width for this I bit measured at  $V_{ref}$ , as a function of cable length. Figures 4 and 5, which show the falling and rising slopes of the pulse measured at  $V_{ref}$  as a function of cable length, were based on these ASTAP simulations. Figure 6 shows the dc-voltage shift which causes the measured pulse width to exceed specifications. This pulse shift corresponds to the noise margin when the correlation coefficient is maximum,  $\rho = 1$ . A noise correlation coefficient of 1 implies that the same noise appears at both ends of the pulse, which is equivalent to having the received pulse shifted by the noise voltage, since a dc shift looks like the same noise voltage at both the rising and the falling edges of the pulse. Table 2 summarizes Figs. 4, 5, and 6, where noise margin is given for this case of perfectly correlated noise  $(\rho = 1).$ 

A more general analysis is presented in the next section.

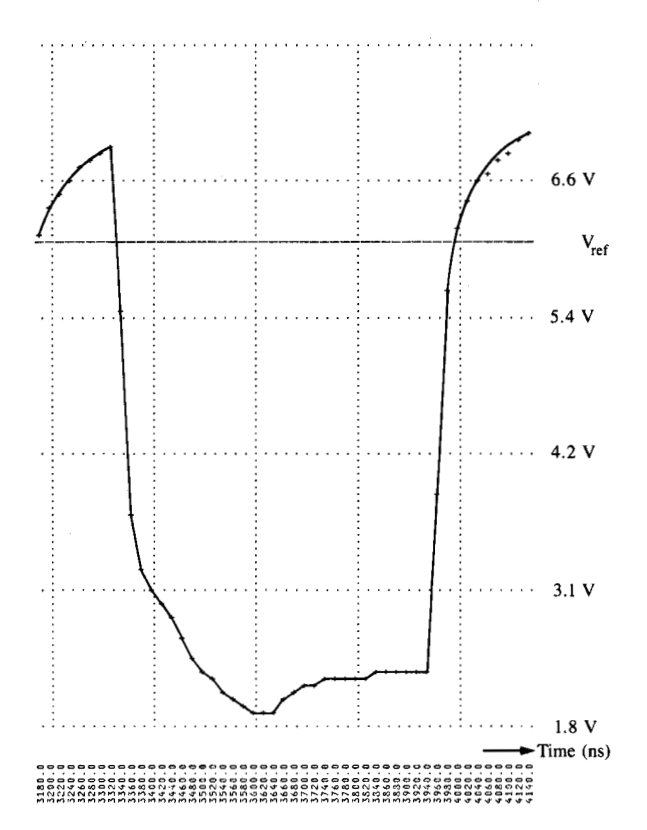


Figure 2 ASTAP simulation of worst-case pulse.

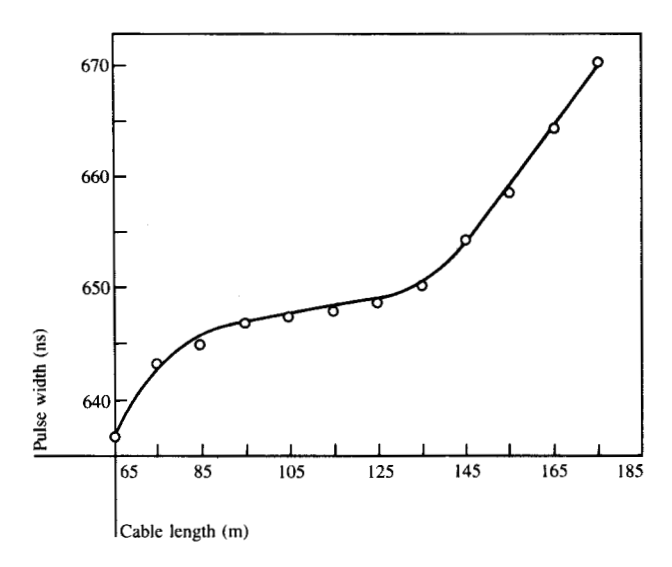


Figure 3 Pulse width vs cable length plot.

### 4. Effect of noise in a PWM system

The analysis of the PWM system performance is based upon an evaluation of the probability of error. An error in this case is defined as occurring when the pulse spread and noise on the cable cause the detected pulse at the receiver to be out of specification.

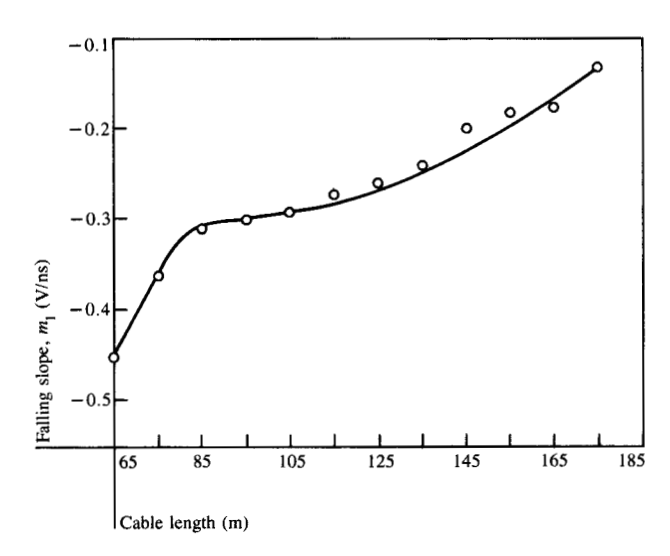


Figure 4 Falling slope  $m_1$  of received signal at  $V_{ref}$ 

Table 2 Pulse widths, falling and rising slopes, and noise margins as functions of cable length.

Cable length (m)	Pulse width (ns)	Falling slope m <sub>i</sub> (V/ns)	Rising slope m <sub>2</sub> (V/ns)	Noise margin (V)
65	637	-0.457	0.023	0.72
75	643	-0.3625	0.0195	0.5
85	645	-0.306	0.0176	0.412
95	647	-0.3	0.0182	0.395
100	647	-0.29	0.0176	0.382
105	647.5	-0.29	0.018	0.38
110	648	-0.28	0.018	0.379
115	648	-0.27	0.018	0.377
120	648	-0.27	0.018	0.376
125	648.5	-0.263	0.018	0.375
130	649	-0.249	0.019	0.374
135	650	-0.234	0.020	0.373
140	652	-0.2174	0.020	0.334
145	654	-0.195	0.019	0.275
150	656	-0.186	0.018	0.2302
155	658	-0.18	0.018	0.196
160	660	-0.18	0.014	0.135
165	664	-0.176	0.014	0.0989
170	667	-0.169	0.013	0.0318
175	670	-0.109 -0.126	0.011	0.0318
180	674	-0.120 $-0.121$	0.007	U

Consider the arbitrary pulse p(t) and the pulse plus noise p(t) + n(t) as shown in Fig. 7, where n(t) is a Gaussian random variable. The pulse with added noise crosses the reference  $V_{\text{ref}}$  at different points from the pulse with no noise. The time differences on the falling and rising edges are  $\Delta t_1$  and  $\Delta t_2$ , respectively. When these wave shapes are reason-

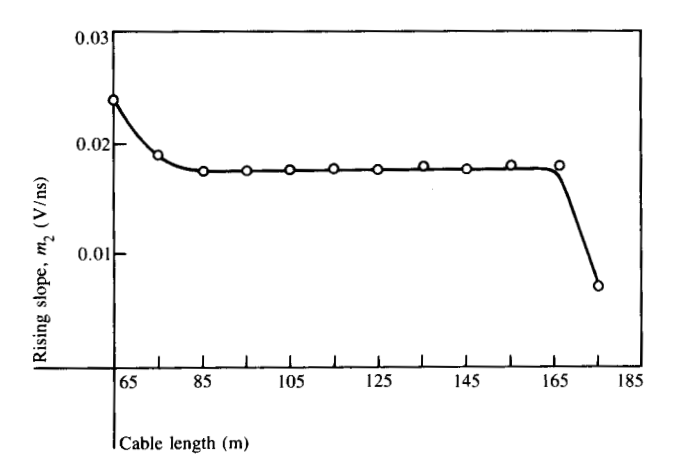


Figure 5 Rising slope  $m_2$  of received signal at  $V_{ref}$ 

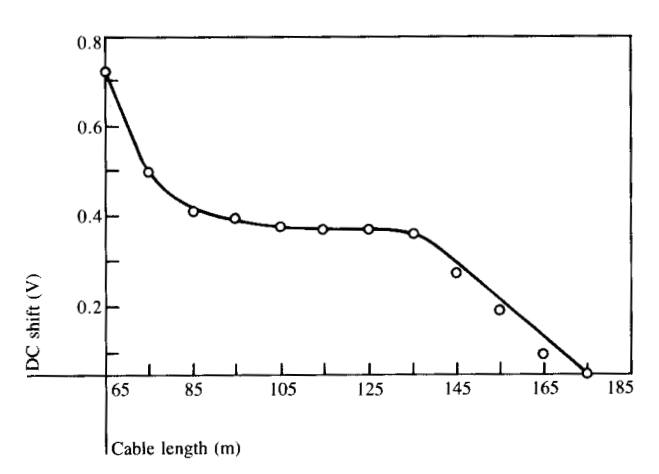


Figure 6 DC shift to exceed the pulse width, as a function of cable length.

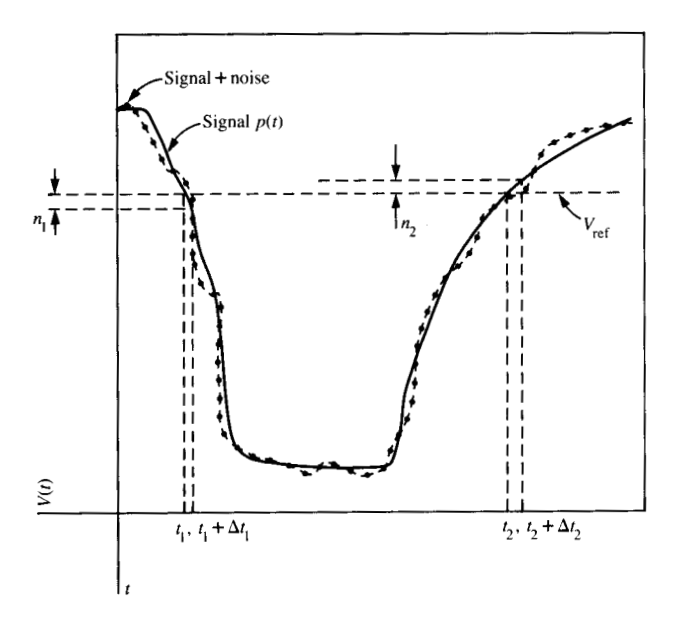


Figure 7 Pulse signal plus noise in a PWM system.

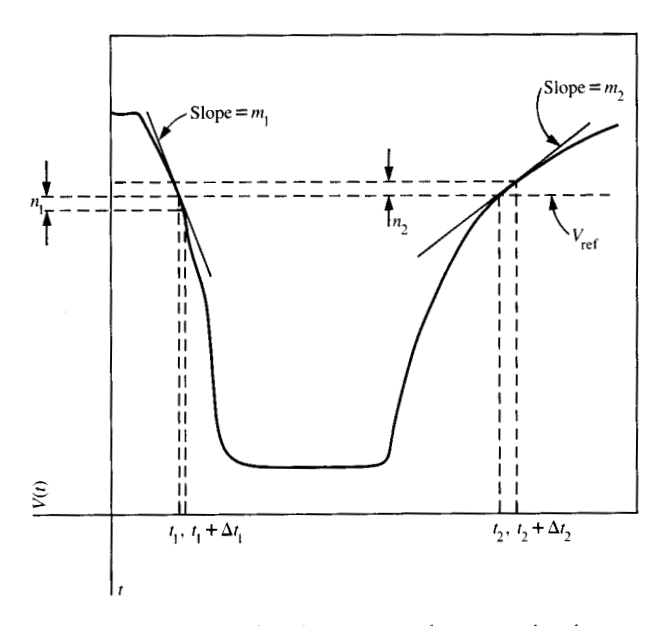


Figure 8 Timing error based on constant-slope approximation.

ably linear near  $V_{\rm ref}$ , a significant simplification of the analysis can be achieved. The waveform presented in Fig. 2 shows the rising and falling edges of the pulse in the vicinity of  $V_{\rm ref}$ . Since the assumption of linearity need only be valid in the region of  $V_{\rm ref}$ , this engineering approximation can be used here. Continuing with the analysis under the assumption of linearity, we define the falling and rising slopes as  $m_1$  and  $m_2$ , respectively, as shown in Fig. 8. Then the relationship between the noise and the shift in the  $V_{\rm ref}$  crossing of the signal is

$$n_1 = -m_1 \triangle t_1 \tag{1}$$

and

$$n_2 = -m_2 \triangle t_2 \,. \tag{2}$$

The pulse width variation is then

$$-\triangle t_1 + \triangle t_2 = \frac{n_1}{m_1} - \frac{n_2}{m_2}. \tag{3}$$

An examination of the actual noise sources in multiplebalanced shielded twisted-pair cable with common-mode noise rejection shows the dominant noise source to be nearend crosstalk. The literature shows that this noise can be treated as uncorrelated noise [2].

435

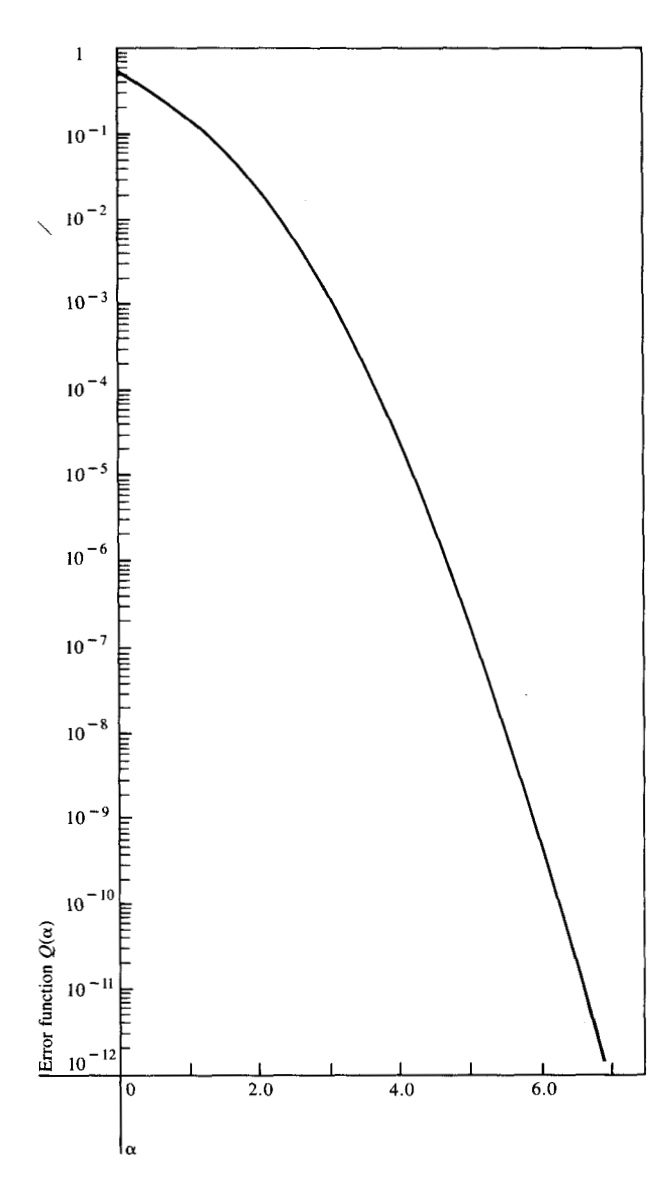


Figure 9 The error function  $Q(\alpha)$ .

Proceeding with the assumption that  $n_1$  and  $n_2$  are zero mean random variables with variances of  $\sigma_1^2$  and  $\sigma_2^2$  respectively, and

$$\frac{\mathrm{E}\left[n_{1}n_{2}\right]}{\sigma,\,\sigma_{2}}=\rho(\tau),$$

where the  $\rho(\tau)$  indicates some possible pulse width dependence of the correlation [3], then

$$\mathbf{E}[-\Delta t_1 + \Delta t_2] = 0 \tag{4}$$

and

$$var(-\Delta t_1 + \Delta t_2) = E[(-\Delta t_1 + \Delta t_2)^2]$$
 (5)

$$= E \left[ \left( \frac{n_1}{m_1} - \frac{n_2}{m_2} \right)^2 \right] \tag{6}$$

$$= E\left[ \left( \frac{n_1}{m_1} \right)^2 - \left( \frac{2n_1n_2}{m_1m_2} \right) + \left( \frac{n_2}{m_2} \right)^2 \right]$$
 (7)

$$=\frac{\sigma_1^2}{m_1^2}-\frac{2\rho(\tau)\sigma_1\sigma_2}{m_1m_2}+\frac{\sigma_2^2}{m_2^2}.$$
 (8)

Now if  $\sigma_1^2 = \sigma_2^2 = \sigma^2$ , then

$$var(-\triangle t_1 + \triangle t_2) = \sigma^2 \left( \frac{1}{m_1^2} - \frac{2\rho(\tau)}{m_1 m_2} + \frac{1}{m_2^2} \right) = \sigma_i^2.$$
 (9)

If  $n_1$  and  $n_2$  are both zero mean Gaussian variables with variance  $\sigma^2$ , then  $-\Delta t_1 + \Delta t_2$  will be a zero mean Gaussian variable with variance  $\sigma_t^2$  as defined in Eq. (9), and the probability of error (i.e., not being within specifications) can be evaluated [4, 5].

The error criterion is given as  $t_{\text{max}}$ , the maximum value for the time between reference crossings for an acceptable pulse. For the pulse with no noise, the time between reference crossings is  $t_{\text{d}}$ . With noise, the apparent pulse width becomes

$$t_{\rm p} = t_{\rm d} - \triangle t_1 + \triangle t_2,$$

where  $t_{\rm p}$  is a random variable since  $\triangle t_{\rm l}$  and  $\triangle t_{\rm 2}$  are random. An error occurs if  $t_{\rm p} > t_{\rm max}$ . The probability of error can be expressed as

$$Pr\{error\} = Pr\{t_p > t_{max}\}$$
 (10)

Or

$$Pr\{error\} = Pr\{(-\triangle t_1 + \triangle t_2) > (t_{max} - t_d)\}.$$
 (11)

Equation (11) can be evaluated given the probability density function of  $(-\triangle t_1 + \triangle t_2)$ . For example, if  $(-\triangle t_1 + \triangle t_2)$  is a Gaussian random variable with a variance of  $\sigma_t^2$ , we could evaluate the probability of error as

$$Pr\{error\} = Pr\{(-\Delta t_1 + \Delta t_2) > (t_{max} - t_d)\}$$

$$= Q\left(\frac{t_{max} - t_d}{\sigma_t}\right), \qquad (12)$$

where  $Q(\alpha)$  is the error function [4, 6] and is defined

$$Q(\alpha) \triangleq \Pr\{X > \alpha\} = \int_{\alpha}^{\infty} \frac{1}{\sqrt{2\pi}} e^{-x^2/2} dx.$$
 (13)

A graph of  $Q(\alpha)$  is presented in Fig. 9. The solution of Eq. (11) requires a knowledge of the noise energy density spectrum and a subsequent mapping of that noise energy into a time crossing.

#### Examples

1. Consider the case of a 150-m cable with the specifications requiring  $t_{\text{max}} = 670$  ns. Table 2 shows the pulse characteristics for various cable lengths and can be used to determine nominal pulse width, and pulse rise and fall

slopes. Note that for this length,  $t_d = 656$  ns,  $m_1 = -0.186$  V/ns, and  $m_2 = 0.018$  V/ns in the vicinity of the threshold crossings. If the noises  $n_1$  and  $n_2$  are normally distributed and uncorrelated, with zero mean and variance  $\sigma^2$ , then from Eq. (9), with  $\rho = 0$ ,

$$\sigma_t^2 = \sigma^2 \left( \frac{1}{m_1^2} + \frac{1}{m_2^2} \right), \tag{14}$$

where  $\sigma_{i}$  is in volts. Thus, from Eqs. (12) and (14),

$$Pr\{error\} = Q\left(\frac{t_{\text{max}} - t_{\text{d}}}{\sigma_t}\right)$$
$$= Q\left(\frac{t_{\text{max}} - t_{\text{d}}}{\sqrt{\sigma^2(1/m_1^2 + 1/m_2^2)}}\right). \tag{15}$$

From the example specifications,

$$t_{\text{max}} - t_{\text{d}} = 670 \text{ ns} - 656 \text{ ns} = 14 \text{ ns},$$

and

$$\frac{1}{m_1^2} + \frac{1}{m_2^2} = \frac{1}{(0.186)^2} + \frac{1}{(0.018)^2} = 3115.$$

$$\sigma_t^2 = \sigma^2(3115)$$
, and  $\sigma_t = \sigma\sqrt{3115} = 55.8\sigma$ , resulting in

$$\Pr\{\text{error}\} = Q\left(\frac{14}{55.8\sigma}\right) = Q\left(\frac{0.25}{\sigma}\right). \tag{16}$$

2. If the correlation  $\rho$  is changed from 0 to 1, Eq. (9) becomes

$$\sigma_t^2 = \left(\frac{1}{m_1^2} - \frac{2}{m_1 m_2} + \frac{1}{m_2^2}\right) \sigma^2$$
$$= (28.9 + 597 + 3086) \sigma^2, \text{ and}$$

 $\sigma_t = 60.9\sigma$ , yielding

$$Pr\{error\} = Q\left(\frac{14}{60.9\sigma}\right) = Q\left(\frac{0.2298}{\sigma}\right). \tag{17}$$

By using Eq. (16) or (17), the maximum allowable noise in the twisted copper cable for a display terminal can be determined as a function of the required maximum error rate using the error rate graph, Fig. 9. The required maximum error rate specified for the terminal system is  $10^{-8}$ . From Fig. 9, we see that for this error rate the argument of Q must be 5.6. From Eq. (16), with  $\rho=0$ , then  $\alpha=0.25/\sigma=5.6$ , or  $\sigma=0.044$  V. Similarly, from Eq. (17), with  $\rho=1$ , then  $\alpha=0.2298/\sigma=5.6$ , or  $\sigma=0.041$  V.

3. For simplifying this assumption without using the rising and falling slopes, we can use noise margin  $\triangle v$  from Table 2 to find rms noise. When the noise is perfectly correlated, we can assume that  $\triangle v$  is a shifted voltage as shown in Fig. 10, so that the pulse width at  $V_{\text{ref}}$  is just equal to the specified maximum pulse width (670 ns), that is,  $|n_1| = |n_2| = \triangle v$ ,

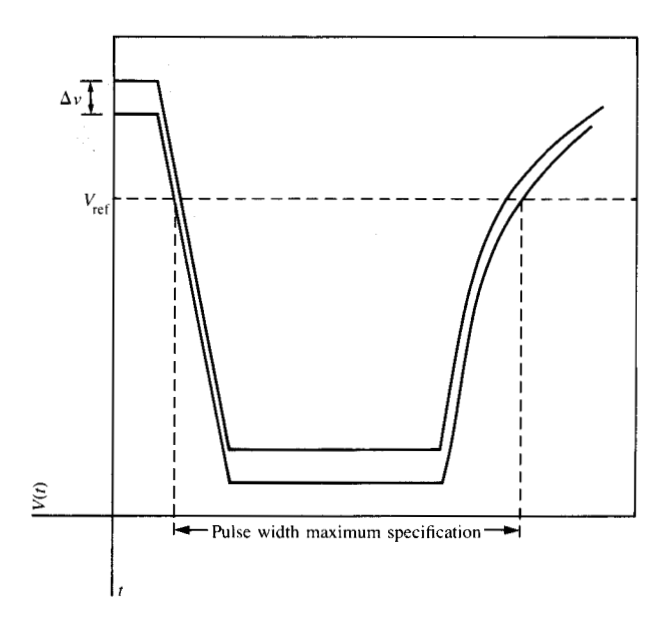


Figure 10 Assumption for shifted level of signal.

$$\sigma_t = \sigma \left( \frac{1}{|m_t|} + \frac{1}{|m_s|} \right)$$
, yielding

$$Q(\alpha) = Q\left(\frac{t_{\max} - t_{\rm d}}{\sigma_t}\right) = Q\left(\frac{\triangle v}{\sigma}\right).$$

We know  $\triangle v$  from Table 2 and  $\alpha$  from Fig. 9. For 150 m, the noise margin  $\triangle v$  is seen to be 0.2302 V. To achieve a  $10^{-8}$  error rate, the allowable noise is found from Fig. 9 to correspond to an  $\alpha$  of 5.6; i.e., the rms noise is the noise margin divided by 5.6:

$$\sigma = \frac{\triangle v}{5.6} = 0.041 \text{ V}.$$

This example shows that the simplifying assumption used in Case 3, that the voltage curve is shifted by the amount of the noise, is equivalent to the assumption that  $\rho=1$ . Returning to Table 2, the noise margin shown can be used to determine the probability of error, given the variance of the noise voltage. The resultant calculation will provide a somewhat conservative estimate, and an upper bound on error rate, without the additional requirement of knowing the details of the noise energy spectrum and computing the noise correlation coefficient.

The computation of error rate as a function of noise voltage has been established for the cable lengths in Table 2 and is tabulated in Fig. 11. As with Table 2, this tabulation is for the case of perfect noise correlation and serves as a conservative estimate of error rate.

437

Figure 11 Table of error rates vs rms noise for various cable lengths.

Using Fig. 11, the allowable cable length can be computed for any input noise voltage and required error rate. As an example, for an input rms noise voltage of 67 mv, we can find the cable length that will support a  $10^{-8}$  error rate in two steps:

- 1. Find the rms voltage greater than or equal to 0.067 V in the 10<sup>-8</sup> error rate column of Fig. 11.
- The cable length for this rms noise is in the same row at the left in Fig. 11. For this example, 125 m is the maximum cable length.

The data from figure 11 is plotted on a semi-log scale in Fig. 12 in terms of probability of error vs rms noise.

#### 5. Simplifying assumptions

When the effect of correlation on system performance is small, computation of error due to noise can be simplified greatly by assuming that the correlation coefficient  $\rho = 1$ . Remember that a noise correlation coefficient of 1 implies that the same noise appears at both ends of the pulse, which is equivalent to having the received pulse shifted by the noise voltage. Figure 10 shows a pulse shifted in voltage so that the pulse width at detection threshold  $(V_{ref})$  is just equal to the specified maximum pulse width. The voltage shift  $\triangle v$ required to increase the pulse width at  $V_{ref}$  to the specification is the noise voltage margin of the system. Since this simplifying assumption is always somewhat conservative, it can be safely used. In addition, it can be accurately used whenever the total dependence on correlation is small. Since the effect of noise on detected pulse width manifests itself through the rising and falling slopes of the detected waveform, a significant difference between rise and fall times (about 10 to 1) guarantees low dependence on correlation. Note that this assumption is independent of the assumption on linearity and can be used on any waveforms with monotonic rise and fall times.

#### 6. Performance evaluation

The performance of a PWM system can be evaluated for any  $\rho$  in the following steps:

- 1. For a given line length, determine the (no noise) pulse parameters  $t_d$ ,  $m_1$ , and  $m_2$  as shown in Table 2 from the ASTAP simulation.
- 2. Compute  $\sigma_s^2$  from Eq. (9), in terms of rms noise voltage.
- 3. Making the Gaussian assumption on the noise, use Eq. (12) to evaluate the probability of an error based on the value of  $t_{max}$ .

Again, the probability of error rate can be found directly in Fig. 11, using the conservative assumption that

$$|n_1| = |n_2| = \triangle v, \qquad \rho = 1.$$

without following steps (1) through (3). The data from Fig. 11, plotted in Fig. 12, show the maximum allowable rms noise voltage versus cable length for values of probability of error between  $10^{-1}$  and  $10^{-8}$ . There are eight curves for  $\rho=1$  (perfectly correlated). The system designer can use this set of curves for specifying cable lengths, noise levels, and/or probability of error. Positive correlation degrades the system performance. Therefore, the probability of error for any given cable length can be conservatively computed by the probability of error equation. Experimental verification of these results is in progress.

#### Summary

This paper has described the analysis and evaluation of the tolerance to noise of a PWM system. Practical considerations were introduced to simplify the analysis, and specific examples were given. Although the motivation for this work was the understanding of IBM display-terminal signal transmission in the presence of noise, the results can be applied to any PWM system. In particular, the simplified approach can be used to get a quick and somewhat conservative bound on acceptable noise, independent of the received pulse wave shape and input noise spectrum, while the detailed analysis can be used to obtain a more exact solution.

#### Acknowledgment

We wish to thank Stephen Townes of the Electrical Engineering Department at North Carolina State University for his technical contributions to the analysis reported here.

#### References

- Installed User Program, Advanced Statistical Analysis Program (ASTAP) Program Reference Manual, Program No. 5796-PBH, available through IBM branch offices.
- Transmission System For Communications, Rev. 4th Ed., by staff members of Bell Telephone Laboratories, Murray Hill, NJ, 1971; Ch. 11.
- William Feller, An Introduction to Probability Theory and Its Applications, Volume I, Third Edition, John Wiley & Sons, Inc., New York, 1968.

- 4. A. Bruce Carlson, Communication Systems, McGraw-Hill Book Co., Inc., New York, 1975, pp. 75–79.
- R. E. Ziemer and W. H. Tranter, Principles of Communications: System, Modulation, and Noise, Houghton Mifflin Co., Boston, 1976
- H. Taub and D. L. Schilling, Principles of Communication Systems, McGraw-Hill Book Co., Inc., New York, 1971.

Received January 25, 1983; revised April 28, 1983

Robert D. Love IBM Communication Products Division, P.O. Box 12195, Research Triangle Park, North Carolina 27709. Mr. Love is an advisory engineer in the network products technology group currently engaged in the design and analysis of local area networks. Before joining IBM, he worked as a microwave engineer at Wheeler Laboratories, Great Neck, New York, from 1963 to 1966, and on cryogenic parametric amplifier design at Control Data Corporation, Melville, Long Island, New York, from 1966 to 1968. He joined IBM in 1968 in the Federal Systems Division at Gaithersburg, Maryland, where he worked in microwave systems design. In 1971 he moved to Manassas, Virginia, where he was involved in various aspects of LSI and VLSI logic design, and design automation system development. He spent 1978-1980 in Kingston, New York, working on VLSI system design and distributed system planning. He moved to North Carolina and his present assignment in 1981. He received his B.S. in electrical engineering from Columbia University, New York, in 1963, and his M.S. in electro-physics from the Polytechnic Institute of Brooklyn in 1968. Mr. Love holds two patents and has reached the Second Invention Achievement Level. He is a member of the Institute of Electrical and Electronics Engineers.

David In-Hwan Park IBM Communication Products Division, P.O. Box 12195, Research Triangle Park, North Carolina 27709. Mr. Park is a senior associate engineer in the Local Area

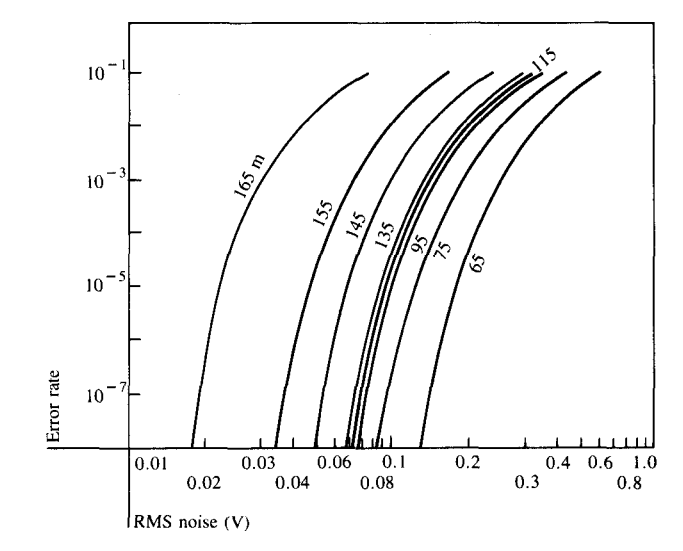


Figure 12 Graph of error rates vs rms noise for various cable lengths.

Network Assurance Department. He joined IBM in Raleigh, North Carolina, in 1978 and worked on X.21 network test tool development. Later he was involved in electrically alterable ROM writer assurance. Since 1981, he has been involved in local area network assurance. Mr. Park received the B.S. in 1976 and the M.S. in 1978 from the University of South Carolina in Columbia, both in the field of electrical engineering. Currently, he is enrolled in the graduate work study program at North Carolina State University in Raleigh to obtain his Ph.D. in electrical and computer engineering. He is a member of the Institute of Electrical and Electronics Engineers and Tau Beta Pi.